Supplementary Information for

Thermal Dissociation of Inter-layer Excitons in $MoS_2/MoSe_2$ Hetero-bilayers

Shinichiro Mouri,[1,4] Wenjin Zhang,[1] Daichi Kozawa,[1] Yuhei Miyauchi,[1] Goki Eda[2,3]

and Kazunari Matsuda[1]

[1]*Institute of Advanced Energy, Kyoto University, Uji, Kyoto 611-0011, Japan*

[2]*Department of Chemistry, National University of Singapore, 3 Science Drive 3, Singapore 117543, Singapore*

[3]*Graphene Research Centre, National University of Singapore, 6 Science Drive 2, Singapore 117546, Singapore*

[4]*Department of Electrical and Electronic Engineering, Ritsumeikan University, Kusatsu, 525–8577, Japan*

S1 PL intensity and peak position of the inter-layer excitons in the 1L-MoS_2/1L-$MoSe_2$ hetero-structure at various temperatures

The PL spectrum of the 1L-MoS_2/1L-$MoSe_2$ hetero-bilayer can be decomposed into three major components from the intra-layer excitons in MoS_2, $MoSe_2$, and the inter-layer excitons, and each component has fine structure. Figure S1(a) shows decomposed PL spectra, M_1 (1.63 eV), M_2 (1.59 eV), and M_3 (1.55 eV), corresponding to the emissions of intra-layer excitons, charged excitons (trions), and defect-bound excitons from the $MoSe_2$ layer, respectively. I_1 (1.47 eV), I_2 (1.42 eV), and I_3 (1.38 eV) are also attributed to the PL peaks of inter-layer excitons, inter-layer trions, and inter-layer defect-bound excitons. Figure S1(b) shows the PL intensities of the intra-layer excitons in MoS_2 (blue squares) and $MoSe_2$ (black triangles), and inter-layer excitons (peak I, red circles) in the 1L-MoS_2/1L-$MoSe_2$ hetero-bilayer, plotted as functions of temperature. Figure S1(c)

shows the temperature dependences of the emission energies of the intra-layer excitons in MoS_2 (blue squares) and $MoSe_2$ (black triangles), and inter-layer excitons (peak I, red circles). The energies of these PL peaks can be fitted by the Valshni formula

$$E(T) = E(0) - \alpha T^2 / (\beta + T), \qquad \text{(S1)}$$

where the parameters are $E(0)$ = 1.655 eV, α = 9.8 × 10^{-4} eV/K, and β = 327 K for $MoSe_2$, and $E(0)$ = 1.887 eV, α = 4.2 × 10^{-4} eV/K, and β = 500 K for MoS_2.

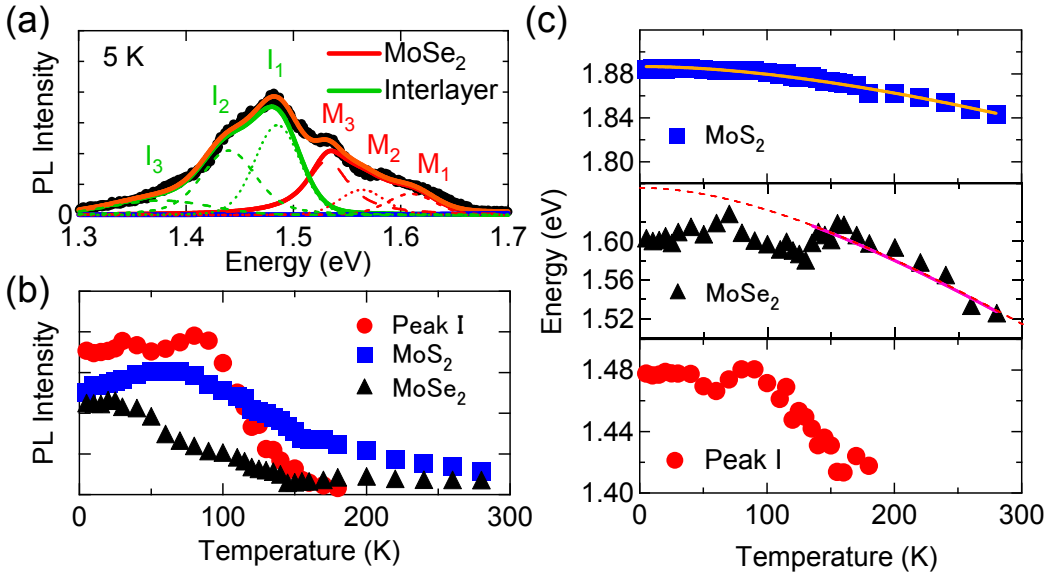

Fig. S1. (a) Decomposed PL spectrum of the 1L-MoS_2/1L-$MoSe_2$ hetero-bilayer measured at 5 K. (b) Temperature dependences of the PL intensities of MoS_2, $MoSe_2$, and peak I. (c) PL energies (peak positions) of MoS_2, $MoSe_2$, and peak I as a function of temperature.

S2 Model of PL intensity quenching based on rate equation analysis

Arrhenius-type quenching is deduced from rate equation analysis based on non-radiative thermal dissociation of the inter-layer excitons. Time-dependent inter-layer exciton population N_I is described as

$$\frac{dN_I}{dt} = G - \gamma_R N_I - \gamma_{NR} N_I, \qquad \text{(S2)}$$

where G is the generation rate of the inter-layer excitons, and γ_R and γ_{NR} represent

radiative and non-radiative decay rates of the inter-layer excitons, respectively. Here we assume that the non-radiative decay process of inter-layer excitons is dominated by the thermal dissociation process into unbounded electrons and holes. Then, the non-radiative decay rate is expressed as

$$\gamma_{\mathrm{NR}} = \gamma_0 \exp(-\frac{E_{\mathrm{a}}}{k_{\mathrm{B}}T}), \tag{S3}$$

where γ_0 is a rate constant and E_{a} is the thermal activation energy of inter-layer excitons, which corresponds to the inter-layer exciton binding energy E_{b}. The steady-state solution of equation (S2) assuming the thermal dissociation process γ_{NR} provides the temperature dependence of the inter-layer exciton PL intensity I_{I} as,

$$I_{\mathrm{I}} \propto \gamma_{\mathrm{R}} N_{\mathrm{I}} = \frac{\mathrm{G}}{1 + \gamma_0 / \gamma_{\mathrm{R}} \exp(-E_{\mathrm{b}} / k_{\mathrm{B}}T)}. \tag{S4}$$

This leads to the eq. (1) in the main text, when A corresponds to $\gamma_0/\gamma_{\mathrm{R}}$. The PL intensity of the inter-layer excitons as a function of temperature is calculated using eq. (S4).

Figure S2(a) shows the calculated inter-layer exciton PL intensity with various exciton binding energies E_{b}, where A is a constant value of 4000. The temperature at which the PL intensity starts to decrease shifts to the higher temperature side with increasing exciton binding energy. Figures S2(b) and (c) show the calculated inter-layer exciton PL intensity with various A, for E_{b} of (b) 0.09 eV and (c) 0.01 eV, respectively. The PL quenching behavior strongly depends on the constant A. The fitting parameters of E_{b} (=93 meV) and A (=4000) are uniquely determined by fitting to the experimental data in Fig. 3(c).

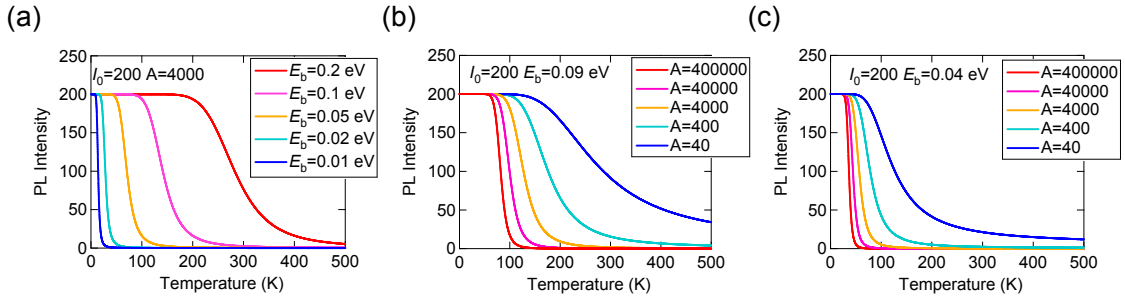

Fig. S2. Temperature dependence of the inter-layer exciton PL intensities for various values of parameters (a) E_b with A = 4000, and (b, c) A with E_b of (b) 0.09 and (c) 0.01 eV, respectively. All the curves are calculated using eq. (2) in the main text.

S3 PL spectra of isolated 1L-$MoSe_2$, 1L-MoS_2, and their hetero-bilayer device at 50 K with an applied gate bias voltage of −10 V

Figure S3 shows PL spectra of the isolated 1L-MoS_2, the isolated 1L-$MoSe_2$, and the 1L-MoS2/1L-MoSe2 hetero-bilayer with an applied bias voltage of −10 V at 50 K. Both the isolated 1L-MoS_2 and 1L-$MoSe_2$ are *n*-type due to unintentionally doped electrons. We observed PL peaks of trions (~1.84 eV) and defects (~1.78 eV) in the isolated 1L-MoS_2, measured at a blue circle position in Fig. 4(a). Only a strong PL peak of trion was observed at ~1.62 eV in the isolated 1L-$MoSe_2$ at a red circle in Fig. 4(a). PL peaks of inter-layer excitons (peak I) and defect-related states from the $MoSe_2$ layer (peak D) were observed at around 1.47 and 1.53 eV, respectively, measured at a yellow circle position in Fig. 4(a).

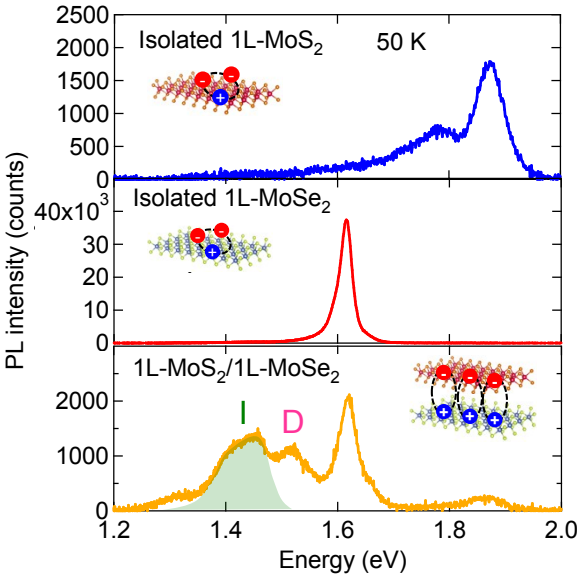

Fig. S3. PL spectra of isolated 1L-MoS_2, 1L-$MoSe_2$, and 1L-MoS_2/1L-$MoSe_2$ hetero-bilayer, at 50 K with an applied gate bias voltage of −10 V.

Figures S4(a) and (b) show the PL spectra of the 1L-MoS_2/1L-$MoSe_2$ hetero-bilayer measured at gate voltages of (a) −90 V and (b) −10 V, and their decomposition into the PL peaks from the inter-layer exciton (I: ~1.47 eV), defect-bound exciton in 1L-$MoSe_2$ (D: ~1.51 eV), trion (X^-: ~1.62 eV) and exciton (X: ~1.65 eV) in 1L-$MoSe_2$, and trion in 1L-MoS_2 (~ 1.87 eV).

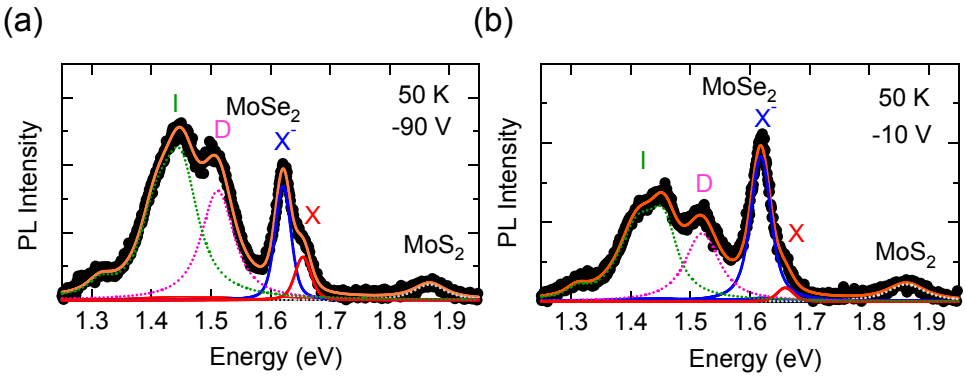

Fig. S4. (a,b) PL spectra of the 1L-MoS_2/1L-$MoSe_2$ hetero-bilayer and its decomposition at (a) −90 V and (b) −10 V.

S4 Law of mass action and estimation of the carrier density of $MoSe_2$

The carrier density of 1L-$MoSe_2$ in the hetero-bilayer is estimated from the spectral weight of charged excitons (trions) and excitons based on the framework of the mass action law. The population ratio between the exciton and trion is described as follows,

$$\frac{N_X n_e}{N_{X^-}} = Bk_B T \exp(-\frac{E_b}{k_B T}), \quad \text{(S5)}$$

where N_x and N_{x^-} are the exciton and trion population, k_B is the Boltzmann constant, n_e is the doped electron density, and E_b is the binding energy of trion, ~30 meV for 1L-$MoSe_2$ and ~18 meV for 1L-MoS_2. The coefficient B in eq. (S5) is described as,

$$B = \frac{4\pi m_X m_e}{\pi \hbar^2 m_{X^-}}, \quad \text{(S6)}$$

where m_e, m_X, and m_{X^-} are effective masses of the electron, exciton, and trion, respectively. The coefficient B is 6.2×10^{11} and 4.1×10^{11} $meV^{-1}cm^{-2}$ for 1L-$MoSe_2$ and 1L-MoS_2, respectively. The normalized spectral weight of trion by the total PL intensity, I_{x^-}/I_{total}, is expressed as,

$$\frac{I_{X^-}}{I_{total}} \approx \frac{Cn_e}{1+Cn_e}, \quad \text{(S7)}$$

where $C = (\gamma_{X^-}/\gamma_X)/(Bk_B T e^{-E_b/k_B T})$ is a constant, 9.4×10^{-12} and 6.7×10^{-11} cm^2 for 1L-MoS_2 and 1L-$MoSe_2$, respectively. γ_x (γ_{x^-}) is the radiative decay rate of excitons (trions). Here we assumed that the ratio γ_{x^-}/γ_x is 0.15, which is consistent with the experimentally obtained results.[S2,S3] Then, we derived the relation between the carrier density and the spectral weight, as shown in Fig. S5(a). The trion spectral weight I_{x^-}/I_{total} changes with the gate voltage as shown in Fig. S5(b). Using these two results, we could estimate the relation between the carrier density and the applied gate voltage as shown in

the lower panel of Fig. 4(d).

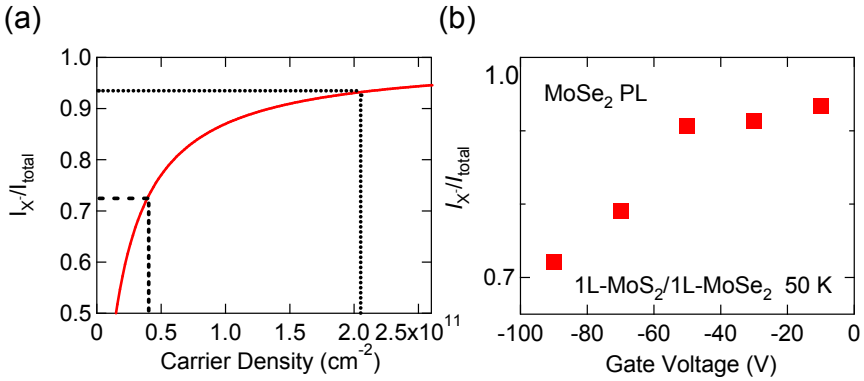

Fig. S5. (a) Calculated trion spectral weight of 1L-$MoSe_2$ based on mass action law at 50 K. (b) Measured trion spectral weight of 1L-$MoSe_2$ for various gate voltages.

S5 PL spectra of 1L-MoS_2 in the hetero-bilayer under gating conditions

Figure S6 shows the PL spectra of the 1L-MoS_2 in the 1L-MoS_2/1L-$MoSe_2$ hetero-bilayer under various gate voltages. The intra-layer exciton PL intensity is very small even at a negative gate voltage, as shown in Fig. S6. The large trion spectral weight (>0.95) suggests a high electron density above 5×10^{12} cm^{-2} in 1L-MoS_2.

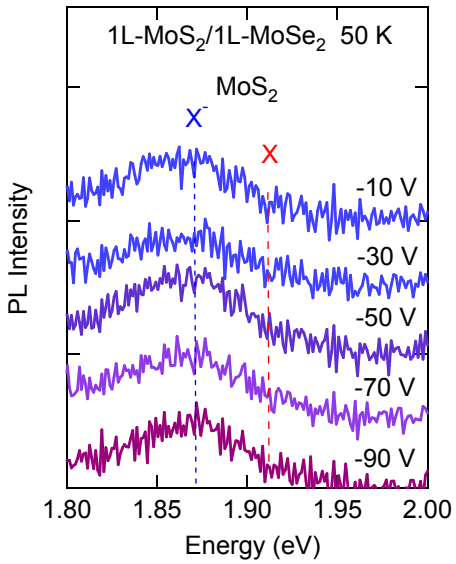

Fig. S6. PL spectra of the 1L-MoS_2 in the hetero-bilayer for various gate voltages at 50 K.

REFERENCES

[S1] Ross, J. S.; Wu, S.; Yu, H.; Ghimire, N. J.; Jones, A. M.; Aivazian, G.; Yan, J.; Mandrus, D. G.; Xiao, D.; Yao, W.; Xu, X. *Nat. Commun.*, 2013, **4**, 1474.

[S2] Mouri, S.; Miyauchi, Y.; Matsuda, K. *Nano Lett.,* 2013, **13**, 5944−5948.

[S3] Robert, C.; Lagarde, D.; Cadiz, F.; Wang, G.; Lassagne, B.; Amand, T.; Balocchi, A.; Renucci, P.; Tongay, S.; Urbaszek, B.; Marie, X. *Phys. Rev. B*, 2016, **93**, 205423.